letters to nature

ture. The integrated PL also increases with temperature in the same manner as the EL, indicating that the temperature dependence is intrinsic to the recombination, rather than the injection mechanism. The strong temperature quenching of PL and EL in most semiconductors is primarily the result of the strong temperature dependence of the competing non-radiative routes—the band-to-band transition is relatively temperature-independent. In our case spatial localization of the radiative carrier population decouples it from any non-radiative recombination occurring elsewhere, thus eliminating the luminescence quenching. A full understanding of the form of the weak increase of the integrated intensity with temperature seen requires further investigation; it could be associated with increased scattering within the confined carrier populations and the increase in the effective density of band states with temperature. We have also carried out EL frequency-resolved measurements that give a device response time, at room temperature, of $18 \pm 2 \, \mu s$. The PL and EL are both superlinear with excitation power and drive current respectively, meaning that the device improves further as we drive the device harder. In ref. 9 a similar dependence of the luminescence intensity is attributed, owing to a shift in emission wavelength, to sample heating. However, in our case, no such shift is observed.

The external quantum efficiency of our unpackaged planar device has been measured, based only on the light emitted just through the back window. At a 100 mA forward current the emitted light is $19.8 \, \mu W$ giving an external quantum efficiency of $(2.0 \pm 0.1) \times 10^{-4}$ at room temperature. We also obtain significant edge emission from the device, of a further $80 \, \mu W$, but this is not included in our estimate of the quantum efficiency above. Taking it into account, our device has a quantum efficiency of 10^{-3}. The emitted power from the face of the device was measured by placing it immediately adjacent to a large-area calibrated power meter. The power meter is an Ophir Laser Star fitted with a PD300 IR head; the instrument is certificated and calibrated with standards traceable to the National Institute of Standards. Our front emitting devices have the same efficiencies as the back emitting devices. For comparison, commercially available GaAs infrared LEDs have typical external efficiencies of 10^{-2}. However, commercial packing of LEDs, in particular by minimizing the considerable internal reflection losses of the planar device and by collecting the edge emission, can improve the external efficiency by up to a factor of about 15. Our first, non-optimized devices are therefore already within a factor of 3 or so of the efficiencies achieved in conventional optimized LED devices.

We believe that the device demonstrated is the most likely candidate currently for implementing efficient light sources in silicon. Such a device would also form the basis for the development of an injection laser based on the same principles but with the incorporation of an optical cavity. The approach itself is not limited to silicon but could be applied to other materials, particularly other indirect materials and silicon alloys. For example, going from germanium to silicon to silicon carbide could produce devices, using the same approach, that could span the near-infrared region, including the 1.3 μm and 1.5 μm wavelength regions of the spectrum, important for optical fibre communications, and up to the ultraviolet region. □

1. European Commission Technology Roadmap—Optoelectronic Interconnects for Integrated Circuits (eds Forchel, A. & Malinverni, P.) (Office for Official Publications of the European Communities, Luxembourg, 1998).
2. Hirschman, K. D., Tybskov, L., Duttagupta, S. P. & Fauchet, P. M. Silicon-based visible light-emitting devices integrated into microelectronic circuits. Nature 384, 338–341 (1996).
3. Lu, Z. H., Lockwood, D. J. & Baribeau, J.-M. Quantum confinement and light emission in SiO2/Si superlattices. Nature 378, 258–260 (1995).
4. Komoda, T. et al. Visible photoluminescence at room temperature from microcrystalline silicon precipitates in SiO2 formed by ion implantation. Nucl. Instrum. Methods B 96, 387–391 (1995).
5. Zheng, B. et al. Room-temperature sharp line electroluminescence at λ = 1.54 μm from an erbium-doped, silicon light-emitting diode. Appl. Phys. Lett. 64, 2842–2844 (1994).
6. Vescan, L. & Stoica, T. Room-temperature SiGe light-emitting diodes. J. Luminescence 80, 485–489 (1999).
7. Leong, D., Harry, M., Reeson, K. J. & Homewood, K. P. A silicon/iron disilicide light-emitting diode operating at a wavelength of 1.5 μm. Nature 387, 686–688 (1997).
8. Tybskov, L., Moore, K. L., Hall, D. G. & Fauchet, P. M. Intrinsic band-edge photoluminescence from silicon clusters at room temperature. Phys. Rev. B 54, R8361–R8364 (1996).
9. Sveinbjörnsson, E. O. & Weber, J. Room temperature electroluminescence from dislocation rich silicon. Appl. Phys. Lett. 69, 2686–2688 (1996).
10. Hirth, J. P. & Lothe, J. Theory of Dislocations 2nd edn, 63 (John Wiley & Sons, New York, 1982).

....

Dating of the oldest continental sediments from the Himalayan foreland basin

Yani Najman*§, Malcolm Pringle†, Laurent Godin‡§ & Grahame Oliver¶

* Fold and Fault Research Project, Department of Geology and Geophysics, University of Calgary, 2500 University Drive NW, Calgary, AB, Canada T2N 1N4
† Scottish Universities Environmental Research Centre, Scottish Enterprise Technology Park, Rankine Avenue, East Kilbride G75 0QF, UK
‡ Department of Earth Sciences, Oxford University, Parks Road, Oxford OX1 3PR, UK
¶ Crustal Geodynamics Group, School of Geography and Geosciences, Purdie Building, The University, St Andrews, Fife KY16 9ST, UK

....

A detailed knowledge of Himalayan development is important for our wider understanding of several global processes, ranging from models of plateau uplift to changes in oceanic chemistry and climate[1–4]. Continental sediments 55 Myr old found in a foreland basin in Pakistan[5] are, by more than 20 Myr, the oldest deposits thought to have been eroded from the Himalayan metamorphic mountain belt. This constraint on when erosion began has influenced models of the timing and diachrony of the India–Eurasia collision[6–8], timing and mechanisms of exhumation[9,10] and uplift[11], as well as our general understanding of foreland basin dynamics[12]. But the depositional age of these basin sediments was based on biostratigraphy from four intercalated marl units[5]. Here we present dates of 257 detrital grains of white mica from this succession, using the ^{40}Ar–^{39}Ar method, and find that the largest concentration of ages are at 36–40 Myr. These dates are incompatible with the biostratigraphy unless the mineral ages have been reset, a possibility that we reject on the basis of a number of lines of evidence. A more detailed mapping of this formation suggests that the marl units are structurally intercalated with the continental sediments and accordingly that biostratigraphy cannot be used to date the clastic succession. The oldest continental foreland basin sediments containing metamorphic detritus eroded from the Himalaya orogeny therefore seem to be at least 15–20 Myr younger than previously believed, and models based on the older age must be re-evaluated.

The Balakot Formation, located in the Hazara–Kashmir Syntaxis of Northern Pakistan, is a continental foreland basin sedimentary sequence that contains detritus eroded from the India–Eurasia suture zone and the metamorphic rocks of the Himalaya[11]. The Balakot Formation overlies the Palaeocene shallow marine Patala Formation (Figs 1 and 2) and consists of a >8-km-thick fossil-free

§ Present addresses: Department of Geology & Geophysics, Edinburgh University, West Mains Road, Edinburgh EH9 3JW, UK (Y.N.); Department of Earth Sciences, Simon Fraser University, 8888 University Drive, Burnaby BC, V5A 1S6, Canada (L.G.).

clastic red bed succession, within which are intercalated four discrete grey fossiliferous marl bands (Fig. 2). Nummulites and assilines biostratigraphy of the marl bands has constrained the succession to 55–50 Myr (latest Palaeocene to Mid Eocene)[5]. On this basis, the Balakot Formation has been interpreted as being by far the oldest continental sedimentary succession in the foreland basin that contains detritus from the Himalayan metamorphic belt; the start of similar sedimentation did not occur elsewhere in the basin until more than 20 Myr later (Fig. 1): from Bangladesh[8], through India[13] to Pakistan, although in the Kohat region of Pakistan there was a brief interlude of continental sedimentation, the 100–150-m-thick Mami Khel deposits, in the late Early Eocene (~50 Myr) before marine conditions resumed[14].

Our new data show that the Balakot Formation is at least 15–20 Myr younger than previously believed. ^{40}Ar–^{39}Ar ages of 257 detrital single white micas separated from nine samples representing the entire thickness of the Balakot Formation show a significant population of micas 36–40 Myr old (Fig. 3a, and Supplementary Information, Table 1). Because a detrital mineral age cannot be younger than its host sediment depositional age, it is clear that the mica ages and biostratigraphic ages of 55–50 Myr deduced from the fossiliferous marl units are incompatible. One explanation for this apparent discrepancy could be that the mica ages do not represent cooling ages characteristic of the original source area but instead have been reset by metamorphism after deposition in the foreland basin and/or low-temperature alteration. We reject this contention, at least for the main 36–40-Myr mode, for the following reasons. First, all of the micas from the young population analysed so far by step-heating techniques (eight in total) show flat plateaux indicating no significant low-temperature alteration (Fig. 3b). (We do note, as expected, that some of the micas >200 Myr old do show some evidence of alteration; the plateaux are not shown. In addi-

tion, it is possible that at least some of the apparently youngest grains analysed by total-fusion techniques, that is, the four grains <32 Myr old in Fig. 3a, have been altered.) Second, electron microprobe traverses of the micas (Supplementary Information) show that ~50% of the micas analysed show no evidence of alteration (as determined by alkali loss) and that, of the remaining 50%, alkali loss is largely confined to grain edges; in most of these latter grains the loss is insubstantial. Last, epizone/greenschist facies conditions (above ~375 °C) are required to reset Ar–Ar age patterns in detrital illite–white mica[15]. Petrographic analysis shows that the Balakot Formation has been subjected to only relatively low grades of burial

Figure 2 Geological map and cross-section of the Balakot Formation, Kaghan Valley, Pakistan. These new data contrast with mapping undertaken by Bossart and Ottiger[5] (compare with their Fig. 8), who interpreted the Balakot Formation as a steeply north-dipping normal stratigraphic succession, with four intercalated fossiliferous marl bands (labelled C–G). Here we show the presence of south dipping strata, folds, faults and high strain zones. The fossiliferous marl bands (labelled C–G, the same annotations as those used by Bossart and Ottiger[5] in their Fig. 8, for easy comparison) outcrop in the core of anticlines or at high strain zones. We therefore interpret the marl bands as part of an underlying formation, now structurally intercalated with the Balakot Formation and exposed by subsequent deformation. Note also that the Patala–Balakot Formation boundary, interpreted by Bossart and Ottiger[5] as a conformable contact, is here interpreted as a thrust contact, on the basis of its tectonized appearance and shear sense indicators. The cross-section was drawn from point 1, through 2 to 3, as shown on the map. The section is located west of marl band sites E and F. Because the structures plunge moderately to the northwest, marl band sites E and F are located below the surface.
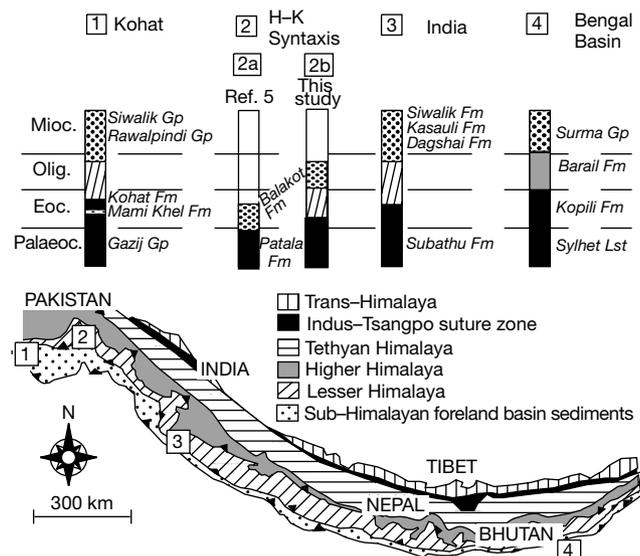

Figure 1 Geological map of the Himalaya showing the location of the study area (2) and a comparison of the foreland basin stratigraphy along strike. Stratigraphic panels are shown from Kohat Region, Pakistan[14] (location and stratigraphic summary (1)), through the Hazara–Kashmir study area (2) (2a, previously accepted stratigraphy, after Bossart and Ottiger[5]; 2b, revised stratigraphy based on this study), to Himachal Pradesh, NW India[13] (3) and the Bengal Basin, Bangladesh[8] (4). Legend for the foreland basin stratigraphic columns: black, shallow marine sediments; grey, deltaic Indian craton-derived sediments; stippled, continental orogen-derived sediments; hatched, no sediments preserved. Note that, with the previously accepted stratigraphy, the Balakot Formation of the Hazara–Kashmir Syntaxis, Pakistan is significantly older than the earliest continental deposits anywhere along strike in the basin.
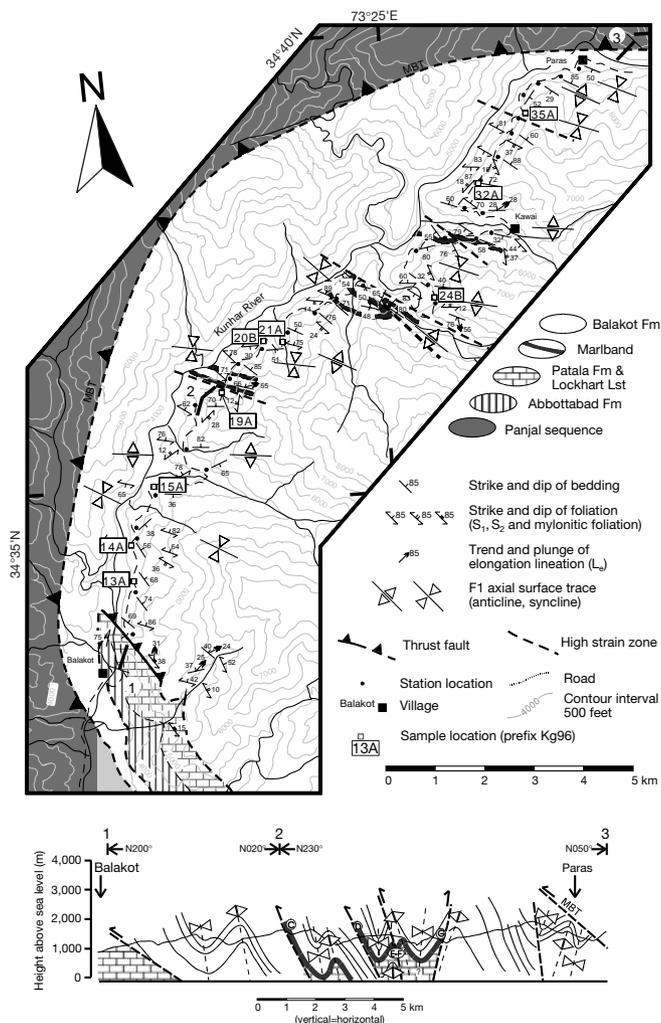
195

metamorphism (prehnite–pumpelyite facies, that is, corresponding to anchizone, ~200–375 °C)[5,16]. This is supported by illite crystallinity measurements, performed on the <2-μm predominantly diagenetic component of the rock, which give an average Hb_{rel} value of 254 ± 43 (Supplementary Information, Table 3). These values correspond to the lower anchizone and upper diagenetic zones, implying that these rocks have been subjected to metamorphic conditions of ~200 ± 50 °C[17–19], which is insufficient to reset ^{40}Ar–^{39}Ar ages in detrital white mica.

We are therefore confident that the ^{40}Ar–^{39}Ar single-crystal mica dates are detrital mineral ages representing the timing of cooling and exhumation in the Himalayan source region, before erosion and deposition with the Balakot Formation, and therefore serve as a robust maximum estimate for the age of sedimentation.

Bossart and Ottiger[5] mapped the Balakot Formation in the Kaghan valley as a steeply north-dipping, homoclinal, normal stratigraphic succession. However, our detailed mapping (Fig. 2), aided by substantial new exposure owing to extensive road building, revealed that the Balakot Formation is intensely folded, with the fossiliferous marl bands outcropping near the cores of anticlines or high-strain zones. These zones are characterized by a penetrative cleavage nearly parallel to bedding, suggestive of intense bedding transposition. Systematic near-vertical slickensides and elongated reduction spots indicate cleavage/parallel slip in the vertical direction. We therefore argue that the marl units are part of an underlying formation, exposed by subsequent deformation related to shear folding and thrusting (Fig. 2b). In addition, we disagree with the interpretation of Bossart and Ottiger[5] that the contact between the Balakot Formation and underlying Palaeocene Patala Formation is conformable. In the region described by Bossart and Ottiger (Behrin Katha), there is insufficient exposure for adequate interpretation. North of Balakot, the Patala Formation outcrops in a highly tectonized zone, imbricated between the west-dipping Abbottabad Formation to the south, and the northeast-dipping Balakot Formation to the north. The Patala Formation is characterized by a penetrative mylonitic foliation with associated down-dip fault striae and displays numerous shear-sense indicators, all suggestive of top-to-the-southwest thrust motion. Near the contact between the Patala and the Balakot formations, the Patala Formation occurs in thin imbricated slivers with the Balakot Formation, and displays sheared-out isoclinal folds. No primary sedimentary features are preserved in the Patala Formation. The contact region is therefore intensely tectonized and we believe that there is inadequate evidence for a conformable contact.

Thus, the petrographic and structural constraints are consistent with the detrital mica ages, showing that the Balakot Formation is no older than 36–40 Myr and is possibly significantly younger. Therefore, the first record of continental foreland basin sediments that contain evidence for erosion from the Himalayan metamorphic belt is >15–20 Myr later than previously believed; models influenced by the older age will need to be re-evaluated in the light of these new data.

Stratigraphic data provide one of the most compelling lines of evidence for the timing and diachrony of collision[7,20]: initiation of orogen-derived foreland basin sedimentation provides a minimum age for orogenic loading of the crust. The marine to continental facies transition in the suture and foreland basin, and variation along strike, has been used to determine the timing and degree of diachrony of collision[6–8], from which estimates of the amount of accommodation of strain by extrusion have been made[6].

Rowley[6] concluded that only in western Zanskar–Hazara was dating (on the oldest syncollisional continental red beds of the Chulung La Formation in Zanskar and the Balakot Formation in Hazara) sufficiently precise to permit the accurate determination of the marine to continental facies transition at 51 Myr. Further east,

stratigraphic data can constrain collision only at <45 Myr, indicating >7 Myr diachrony. However, because the Chulung La Formation is unfossiliferous, its Early Eocene age is based only on its stratigraphic position, unconformably above the Late Paleocene Dibling Limestone, and its assumed but unproved correlation with the fossiliferous marine Kong Slates of that age[21,22]. Hence, Early Eocene is only a robust maximum age for the Chulung La red beds, and the stratigraphic argument rests heavily on the Balakot Formation. Our revised Balakot Formation age of <35 Myr therefore removes all stratigraphic evidence for diachronous collision and also reduces the accuracy of the stratigraphically determined timing of collision (previously taken as 51 Myr)[6] to between 55 Myr (ref. 21) (the youngest marine facies) and <35 Myr.

The earliest record of substantial Himalayan erosion, >15 Myr later than previously believed, forces a reconsideration of the timing and mechanisms of exhumation and uplift, and sedimentary responses to tectonic events. Although it is possible that older sediments are preserved further north beneath the thrust belt or near the base of the Indus or Bengal Fans, the Balakot Formation can no longer be taken as evidence of significant early erosional exhumation synchronous with the initial stages of collision, metamorphism and initiation of a period of rapid cooling, thrusting and extension that began in the Eocene[9,10]. Thus, the relative importance of tectonic exhumation might be increased. Evidence of uplift by 55–50 Myr, as inferred from the interpreted thrust-belt barrier required to explain the contrasting provenance between the previously assumed coeval Chulung La suture zone sediments and the Balakot Formation foreland basin sediments[11], is no longer substantiated.

Our revision of the age and structure of the Balakot Formation affects current models of the early stages of foreland basin evolution. Burbank et al.[12] surmised that basin geometry was affected by changes in the rigidity of the underthrust plate with time. The thickness and age of the Balakot Formation supported the conten-
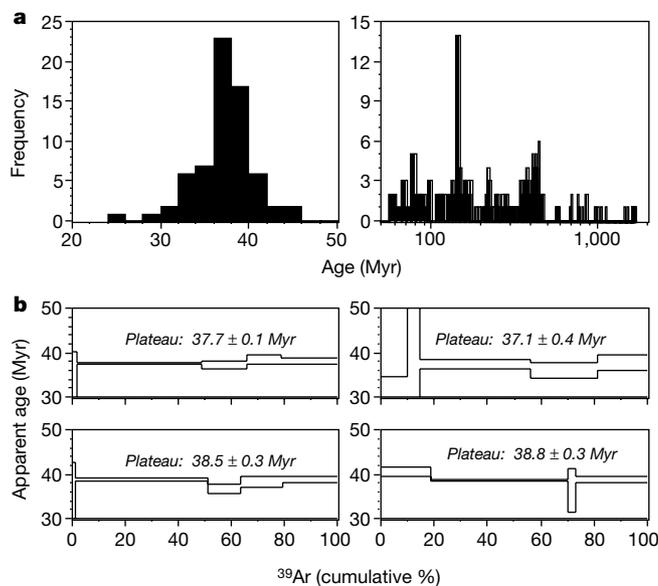

Figure 3 Summary of Ar–Ar analyses of single-crystal detrital white micas from the Balakot Formation sediments, Pakistan. **a**, Distribution of Ar–Ar laser-fusion and step-heating analyses of 257 individual white mica grains from the Balakot Formation, Pakistan. Grains 20–50 Myr old (left panel; 67 crystals) were sorted in 2-Myr-wide intervals; grains 50–2,000 Myr old (right panel; 190 crystals) were sorted in 5-Myr intervals; the analytical error is typically less than the bin width. **b**, Single-crystal Ar–Ar age spectra of four micas from a 36–40-Myr population; each step is drawn 2 s.d. tall. Analytical methods followed Richards et al.[24]

tion that younger and weaker Indian crust subducted during the earliest stages of collision would be reflected in a narrower and deeper basin. This early basin subsided rapidly, with sedimentation rates (calculated from the intercalated marl bands)[5] up to an order of magnitude higher than during later stages of basin evolution in the Neogene[12]. Our documentation of the structure of the Balakot Formation not only substantially decreases its stratigraphic thickness, and hence estimates of the depth of the basin at this time, but also shows that the marl bands cannot be used to determine sedimentation rates of the clastic deposits and therefore that there is no constraint on the early sedimentation and subsidence history of the basin. Our new age for the Balakot Formation negates its use as evidence of early orogenic loading and flexural subsidence, and removes the Hazara–Kashmir syntaxis region from its previously anomalous status to the otherwise basin-wide[13,23] occurrence of a >20 Myr unconformity separating marine and continental facies. □

1. Ruddiman, W. F. & Kutzbach, J. E. Plateau uplift and climate change. *Sci. Am.* **264**, 42–50 (1991).
2. Krishnaswami, S., Trivedi, J. R., Sarin, M., Ramesh, R. & Sharma, K. Strontium isotopes and rubidium in the Ganga–Bramaputra rivers system: Weathering in the Himalaya, fluxes to the Bay of Bengal and contributions to the evolution of oceanic $^{87}Sr/^{86}Sr$. *Earth Planet. Sci. Lett.* **109**, 2443–253 (1992).
3. Richter, F. M., Rowley, D. B. & DePaolo, D. J. Sr isotopic evolution of seawater: the role of tectonics. *Earth Planet. Sci. Lett.* **109**, 11–23 (1992).
4. Houseman, G. & England, P. Crustal thickening versus lateral expulsion in the Indian–Asian continental collision. *J. Geophys. Res.* **98**, 12233–12249 (1993).
5. Bossart, P. & Ottiger, R. Rocks of the Murree Formation in Northern Pakistan: indicators of a descending foreland basin of late Palaeocene to middle Eocene age. *Eclogae Geol. Helv.* **82**, 133–165 (1989).
6. Rowley, D. B. Age of initiation of collision between India and Eurasia: A review of stratigraphic data. *Earth Planet. Sci. Lett.* **145**, 1–13 (1996).
7. Rowley, D. B. Minimum age of initiation of collision between India and Eurasia north of Everest based on the subsidence history of the Zhepure mountain section. *J. Geol.* **106**, 229–235 (1998).
8. Uddin, A. & Lundberg, N. Cenozoic history of the Himalayan–Bengal system: Sand composition in the Bengal Basin, Bangladesh. *Geol. Soc. Am. Bull.* **110**, 497–511 (1998).
9. Treloar, P. J., Rex, D. C. & Williams, M. P. The role of erosion and extension in unroofing the Indian Plate thrust stack, Pakistan Himalaya. *Geol. Mag.* **128**, 465–478 (1991).
10. Treloar, P. J. Exhumation of high-grade Indian Plate rocks in North Pakistan: Mechanical implications of a multi-phase process. *Terra Nostra* **2**, 157–158 (1999).
11. Critelli, S. & Garzanti, E. Provenance of the Lower Tertiary Murree redbeds (Hazara–Kashmir Syntaxis, Pakistan) and initial rising of the Himalayas. *Sedim. Geol.* **89**, 265–284 (1994).
12. Burbank, D. W., Beck, R. A. & Mulder, T. The Himalayan foreland basin. In *The Tectonic Evolution of Asia* (eds Yin, A. & Harrison, T. M.) 149–188 (Cambridge Univ. Press, 1996).
13. Najman, Y. M. R., Pringle, M. S., Johnson, M. R. W., Robertson, A. H. F. & Wijbrans, J. R. Laser $^{40}Ar/^{39}Ar$ dating of single detrital muscovite grains from early foreland basin sediments in India: Implications for early Himalayan evolution. *Geology* **25**, 535–538 (1997).
14. Pivnik, D. A. & Wells, N. A. The transition from Tethys to the Himalaya as recorded in northwest Pakistan. *Geol. Soc. Am. Bull.* **108**, 1295–1313 (1996).
15. Clauer, N. & Chaudri, S. Isotopic dating of very low-grade metasedimentary and metavolcanic rocks: techniques and methods. In *Low Grade Metamorphism* (eds Frey, M. & Robinson, D.) 202–226 (Blackwell Science, 1999).
16. Bossart, P. *Eine Neuinterpretation der Tektonik der Hazara Kashmir Syntaxis (Pakistan).* Thesis, ETH Zurich, Switzerland (1986).
17. Kubler, B. La cristallinité de l'illite à les zones tout a fait supérieures du metamorphismé. In *Étages Tectoniques* 105–122. (A la Baconnière, Neuchatel, Switzerland, 1967).
18. Blenkinsop, T. G. Definition of low-grade metamorphic zones using illite crystallinity. *J. Met. Petrol.* **6**, 623–636 (1988).
19. Weber, K. Notes on the determination of illite crystallinity. *Neues Jb. Miner. Monatshefte* **6**, 267–276 (1972).
20. Butler, R. When did India hit Asia? *Nature* **373**, 20–21 (1995).
21. Garzanti, E., Baud, A & Mascle, G. Sedimentary record of the northward flight of India and its collision with Eurasia (Ladakh Himalaya, India). *Geodinim. Acta* **1**, 297–312 (1987).
22. Garzanti, E., Critelli, S & Ingersoll, R. V. Paleogeographic and paleotectonic evolution of the Himalayan range as reflected by detrital modes of Tertiary sandstones and modern sands (Indus transects, India and Pakistan). *Geol. Soc. Am. Bull.* **108**, 631–642 (1996).
23. DeCelles, P. G., Gehrels, G. E., Quade, J. & Ojha, T. P. Eocene–early Miocene foreland basin development and the history of Himalayan thrusting, western and central Nepal. *Tectonics* **17**, 741–765 (1998).
24. Richards, J. P., Noble, S. R. & Pringle, M. S. A revised Late Eocene age for porphyry Cu magmatism in the Escondida Area, Northern Chile. *Econ. Geol.* **94**, 1231–1248 (1999).

Evidence for mantle metasomatism by hydrous silicic melts derived from subducted oceanic crust

Gaelle Prouteau*†, **Bruno Scaillet**‡, **Michel Pichavant**‡ & **René Maury***

* UMR 6538, UBO, 6 avenue Le Gargeu, P.B. 809, 29285 Brest, France
‡ UMR G113, ISTO, 1a rue de la Férollerie, 45071 Orléans, France

The low concentrations of niobium, tantalum and titanium observed in island-arc basalts are thought to result from modification of the sub-arc mantle by a metasomatic agent, deficient in these elements, that originates from within the subducted oceanic crust[1]. Whether this agent is an hydrous fluid[2] or a silica-rich melt[3] has been discussed using mainly a trace-element approach[4] and related to variable thermal regimes of subduction zones[5]. Melting of basalt in the absence of fluid both requires high temperatures and yields melt compositions unlike those found in most modern or Mesozoic island arcs[6,7]. Thus, metasomatism by fluids has been thought to be the most common situation. Here, however, we show that the melting of basalt under both H_2O-added and low-temperature conditions can yield extremely alkali-rich silicic liquids, the alkali content of which increases with pressure. These liquids are deficient in titanium and in the elements niobium and tantalum and are virtually identical to glasses preserved in mantle xenoliths found in subduction zones[6] and to veins found in exhumed metamorphic terranes of fossil convergent zones[7]. We also found that the interaction between such liquids and mantle olivine produces modal mineralogies that are identical to those observed in metasomatized Alpine-type peridotites[8]. We therefore suggest that mantle metasomatism by slab-derived melt is a more common process than previously thought.

A mid-ocean ridge basalt from the Juan de Fuca ridge (Table 1) was reacted between 10 and 30 kbar with bulk H_2O contents of 2 to 10 wt% (see ref. 9 for methods), that is, largely in excess of the H_2O content of metamorphosed basalts, and at temperatures below 1,000 °C. Recent experimental work has shown that melting under these conditions (addition of H_2O, low temperatures) is required to account for the geochemical and physical characteristics of slab melts[9], and approaches the most likely pressure–temperature (P–T) conditions for slab melting (750 °C, 30 kbar) as constrained from thermal modelling[10].

Representative glass (that is, quench melt) compositions are listed in Table 1. In a An–Ab–Or projection (Fig. 1), the glass compositions define a trend parallel to the albite–anorthite join. Glasses

† Present address: Laboratoire de Pétrologie, UPMC, 4 Place Jussieu, 75252, Paris, France.